

## Plasma chemistry modeling for an inductively coupled plasma used for the growth of carbon nanotubes

This article has been downloaded from IOPscience. Please scroll down to see the full text article.

2011 J. Phys.: Conf. Ser. 275 012021

(<http://iopscience.iop.org/1742-6596/275/1/012021>)

View [the table of contents for this issue](#), or go to the [journal homepage](#) for more

Download details:

IP Address: 146.175.13.243

The article was downloaded on 10/02/2011 at 09:16

Please note that [terms and conditions apply](#).

## Plasma chemistry modeling for an inductively coupled plasma used for the growth of carbon nanotubes

Ming Mao and Annemie Bogaerts  
Research group PLASMANT, Department of Chemistry, University of Antwerp  
Universiteitsplein 1, B-2610 Wilrijk-Antwerp, Belgium  
E-mail: annemie.bogaerts@ua.ac.be

### Abstract

A hybrid model, called the hybrid plasma equipment model (HPEM), is used to describe the plasma chemistry in an inductively coupled plasma, operating in a gas mixture of  $C_2H_2$  with either  $H_2$  or  $NH_3$ , as typically used for carbon nanotube (CNT) growth. Two-dimensional profiles of power density, electron temperature and density, gas temperature, and densities of some plasma species are plotted and analyzed. Besides, the fluxes of the various plasma species towards the substrate (where the CNTs can be grown), as well as the decomposition rates of the feedstock gases ( $C_2H_2$ ,  $NH_3$  and  $H_2$ ), are calculated as a function of the  $C_2H_2$  fraction in both gas mixtures.

### 1. Introduction

Carbon nanotubes (CNTs) are gaining increasing interest, due to their unique physical, chemical and electronic properties, giving rise to a variety of (potential) applications, including nanoelectronics, hydrogen storage and field emission devices [1-3]. CNTs can be produced by arc discharges [4], laser ablation [5], chemical vapor deposition (CVD) [6], as well as by plasma enhanced CVD (PE-CVD) [7-25], which appears to be a very promising technology for the synthesis of vertically aligned CNTs, of interest for field emission devices [7]. Several plasma sources have been applied already for the growth of CNTs, including direct current (dc) glow discharges [8-12], capacitively coupled (cc) radiofrequency (rf) discharges [13-15], inductively coupled plasmas (ICPs) [16-22] and microwave (MW) discharges [23-25]. The feedstock gases most often used are  $CH_4$  or  $C_2H_2$ , mixed with either  $H_2$  or  $NH_3$  as so-called etchant gases, i.e., to produce “clean” CNTs, with a limited fraction of amorphous phases.

In this paper, we present results of plasma chemistry modeling performed for an ICP, operating in a mixture of  $C_2H_2$  with either  $H_2$  or  $NH_3$ , in order to investigate the role of the various plasma species created in these gas mixtures, for the CNT growth. The effect of the  $C_2H_2$  fraction in both gas mixtures will be analyzed, and the influence of the two different etchant gases ( $H_2$  or  $NH_3$ ) will be compared.

### 2. Model description

The model used in this work is the so-called hybrid plasma equipment model, developed by Kushner and coworkers [26]. It consists of three main modules, i.e., (i) an electromagnetics module, which calculates the electric and magnetic fields in the reactor, (ii) an electron energy transport module, which simulates the behavior of the (fast) electrons by a Monte Carlo procedure or the Boltzmann equation, and (iii) a fluid kinetics simulation, which treats the other plasma species by conservation equations. A full explanation about this hybrid model can be found in [26].

The focus of the present calculations is on the plasma chemistry. Therefore, a large number of different plasma species have to be taken into account, including electrons, various ions, molecules and radicals, which can react with each other in various collision processes. The plasma species and their reactions considered in the model depend on the gas mixture under study. In [27] we have investigated the detailed plasma chemistry in  $\text{CH}_4/\text{H}_2$ ,  $\text{CH}_4/\text{NH}_3$ ,  $\text{C}_2\text{H}_2/\text{H}_2$  and  $\text{C}_2\text{H}_2/\text{NH}_3$  gas mixtures. The different species taken into account in the model, as well as their reactions, were tabulated in detail [27].

*Table 1: Overview of the species taken into account in the  $\text{C}_2\text{H}_2/\text{H}_2$  model*

<b>Molecules</b>	<b>Radicals</b>	<b>Ions</b>	<b>Electrons</b>
$\text{H}_2$	$\text{H}$	$\text{H}^+, \text{H}_2^+$	$e^-$
$\text{C}_2\text{H}_2$	$\text{C}_2\text{H}, \text{C}_2\text{H}_3, \text{C}_2, \text{CH}_2,$ $\text{CH}, \text{C}$	$\text{C}_2\text{H}_2^+, \text{C}_2\text{H}^+, \text{C}_2\text{H}_3^+, \text{C}_2^+,$ $\text{CH}_2^+, \text{CH}^+, \text{C}^+$	
$\text{C}_4\text{H}_2$	$\text{C}_4\text{H}, \text{C}_4\text{H}_3$	$\text{C}_4\text{H}_2^+, \text{C}_4\text{H}^+, \text{C}_4\text{H}_3^+$	
$\text{C}_6\text{H}_2, \text{C}_6\text{H}_4$	$\text{C}_6\text{H}, \text{C}_6\text{H}_3$	$\text{C}_6\text{H}_2^+, \text{C}_6\text{H}^+, \text{C}_6\text{H}_4^+$	
$\text{C}_8\text{H}_2, \text{C}_8\text{H}_4, \text{C}_8\text{H}_6$	$\text{C}_8\text{H}$	$\text{C}_8\text{H}_2^+, \text{C}_8\text{H}^+, \text{C}_8\text{H}_4^+, \text{C}_8\text{H}_6^+$	
$\text{C}_{10}\text{H}_2, \text{C}_{10}\text{H}_6$	$\text{C}_{10}\text{H}$	$\text{C}_{10}\text{H}_6^+$	
$\text{C}_{12}\text{H}_2, \text{C}_{12}\text{H}_6$	$\text{C}_{12}\text{H}$	$\text{C}_{12}\text{H}_6^+$	

In the present paper, we focus only on the gas mixture of  $\text{C}_2\text{H}_2$  with either  $\text{H}_2$  or  $\text{NH}_3$ . Table 1 summarizes the plasma species included for the  $\text{C}_2\text{H}_2/\text{H}_2$  chemistry, whereas Table 2 presents the extra species added when  $\text{NH}_3$  is used as the dilution gas. In the  $\text{C}_2\text{H}_2/\text{H}_2$  plasma, 31 electron impact reactions, 45 ion-neutral and 29 neutral-neutral reactions are taken into account, whereas an extra number of 43 electron impact reactions, 48 ion-neutral and 67 neutral-neutral reactions were added to the model when  $\text{NH}_3$  is used as the dilution gas. All details about this plasma chemistry can be found in [27].

*Table 2: Overview of the extra species taken into account when  $\text{NH}_3$  is used as the dilution gas*

<b>Molecules</b>	<b>Radicals</b>	<b>Ions</b>
$\text{NH}_3$	$\text{NH}, \text{NH}_2$	$\text{NH}^+, \text{NH}_2^+, \text{NH}_3^+, \text{NH}_4^+$
$\text{N}_2, \text{N}_2\text{H}_2, \text{N}_2\text{H}_4$	$\text{N}, \text{N}^*, \text{N}_2^*, \text{N}_2\text{H}, \text{N}_2\text{H}_3$	$\text{N}_2^+, \text{N}^+$
$\text{HCN}$	$\text{CN}, \text{H}_2\text{CN}$	$\text{HCN}^+$

### 3. Results and discussion

First some general calculation results will be presented for the  $\text{C}_2\text{H}_2/\text{H}_2$  gas mixture, at a ratio of 20/80, a total gas pressure of 50 mTorr, and 100 sccm total gas flow rate. The other operating conditions are 300 W source power, 30 W bias power at the substrate electrode, both applied at an operating frequency of 13.56 MHz. The substrate is heated to 823 K. Next, the effect of the  $\text{C}_2\text{H}_2/\text{H}_2$  gas ratio will be investigated and a comparison will be made with the  $\text{C}_2\text{H}_2/\text{NH}_3$  gas mixture.

### 3.1. General calculation results for the $C_2H_2/H_2$ gas mixture

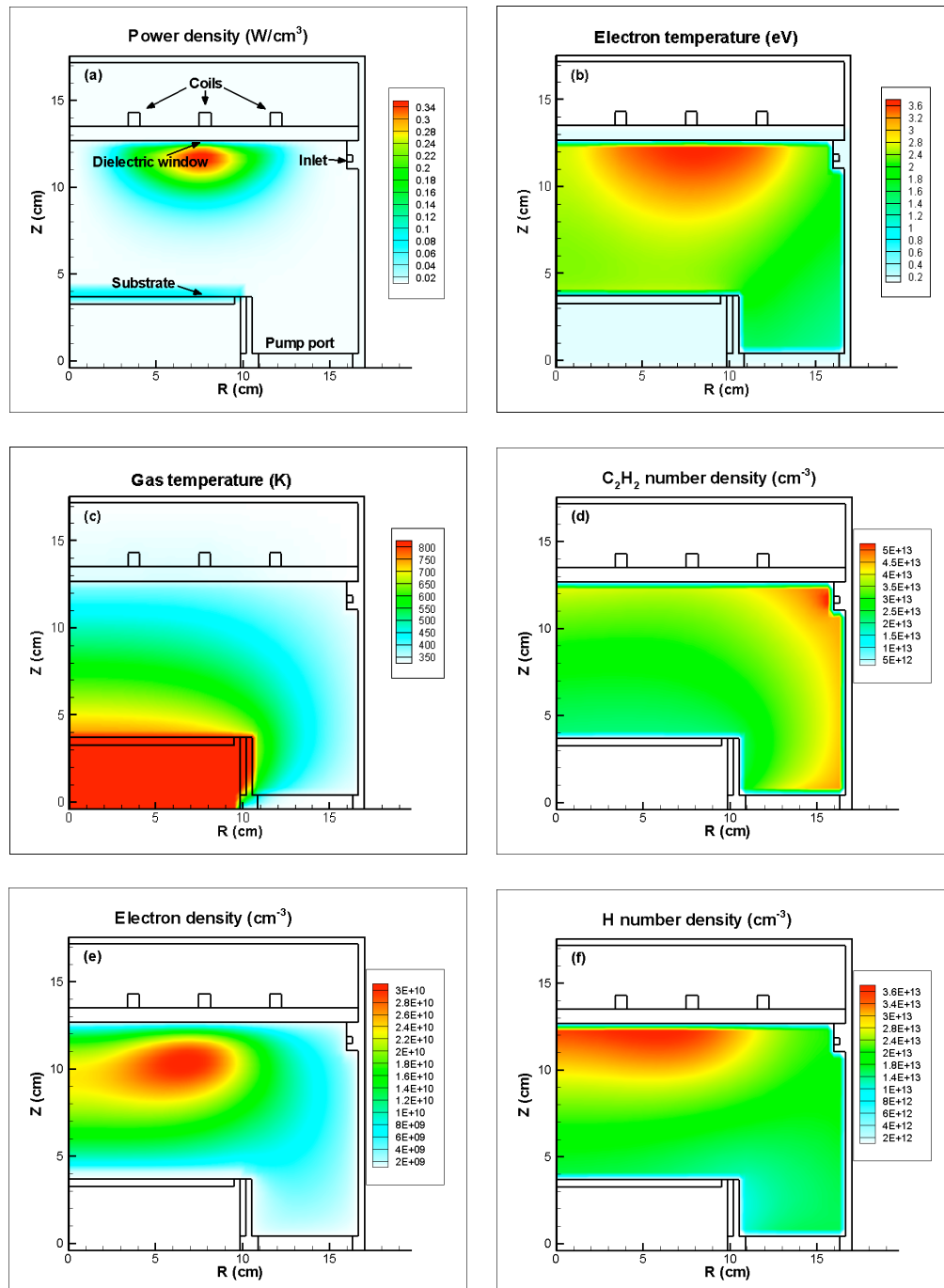


Figure 1: Calculated 2D profiles of (a) the power density, (b) the electron temperature, (c) the gas temperature, (d) the  $C_2H_2$  gas density, (e) the electron density, and (f) the H atom density, in the  $C_2H_2$  gas mixture at a ratio of 20/80, a total gas pressure of 50 mTorr, and a total gas flow rate of 100 sccm. The power applied at the coil and at the substrate is 300 W and 30 W, respectively, both with a frequency of 13.56 MHz. The substrate is heated to 823 K. Only one half plane of the cylindrically symmetrical reactor is shown. The coils, dielectric window, gas inlet, substrate and pump port are indicated in figure (a).

Figure 1 presents calculated 2D profiles of the power density (a), electron temperature (b), gas temperature (c),  $C_2H_2$  gas density (d), electron density (e) and H density (f), in the ICP reactor under study. It is a transformer coupled plasma (TCP) reactor, with a flat coil at the top, which has been applied also experimentally for the growth of CNTs [16,18]. The reactor is cylindrically symmetric, so only one half plane of the reactor is shown. The coil, dielectric window, gas inlet, substrate and pump port are indicated in figure 1(a).

The power density (figure 1(a)) is at maximum just beneath the coil (i.e., the inductive region), and a second maximum is seen in front of the substrate electrode (i.e., the capacitive region). This is logical because the coil power is 300 W, whereas the power applied at the substrate electrode is only 30 W. As a result of this power input, the electrons in the plasma are heated to temperatures of a few eV, as is seen in figure 1(b). Again, the maximum is found beneath the coil. The gas temperature, on the other hand, is at maximum near the substrate, see figure 1(c). Indeed, the substrate is heated to 823 K to enable growth of CNTs [19-22], and the heat is spread out into the plasma. Without substrate heating, the gas would also heat to some extent, but only to about 350 K, as was demonstrated in [28]. Hence, the electron temperature is much higher than the gas temperature, as is typical for a non-LTE plasma.

As a result of this gas temperature profile, the  $C_2H_2$  gas density reaches a minimum in front of the substrate, following the ideal gas law, as is shown in figure 1(d). Further, it is at maximum at the gas inlet, and drops to some extent in the reactor, as it disappears due to ionization and dissociation reactions. The electron density (figure 1(e)) reaches a maximum under the coil, similar to the electron temperature. This means that most of the electron impact reactions (ionization, excitation, dissociation,...) will take place in this region, and that most of the reactive species (i.e., ions, excited species, radicals) will also reach a maximum in this region. This is illustrated in figure 1(f) for the H atom density, but most of the other reactive plasma species indeed exhibit the same profile. The importance of the various reactive species will be discussed in the next section.

### 3.2. Effect of the $C_2H_2/H_2$ gas ratio

The carbon source for CNT growth is defined by the species impinging on the substrate and the decomposition activity on the catalyst surface. Therefore, the fluxes of the various plasma species arriving at the substrate surface are plotted in figure 2, as a function of the  $C_2H_2$  fraction in the gas mixture. It is clear from figure 2(a) that  $H_2$  is the dominant species at low  $C_2H_2$  fraction, whereas  $C_2H_2$  becomes more important at high  $C_2H_2$  fraction. However, the turnover point is not seen at 50%  $C_2H_2$ , but at 80%  $C_2H_2$ , which indicates that  $H_2$  is also formed to a large extent out of  $C_2H_2$ . Besides these two background gases, H atoms are also formed in large amounts, due to various reactions, such as dissociation and ionization of  $C_2H_2$  and  $H_2$ , as is obvious from figure 2(b).

Other important neutral species bombarding the substrate, are  $C_{2n}H_2$  ( $n=2, 3$ ),  $C_6H_4$  and  $C_{2n}H_6$  ( $n=4, 5, 6$ ) (see figure 2(a)), as well as the radicals  $C_{2n}H_3$  ( $n=1, 2, 3$ ) (see figure 2(b)). The fluxes of  $C_{2n}H_2$  ( $n=2, 3$ ) follow the same increasing trend as  $C_2H_2$  upon increasing  $C_2H_2$  gas fraction, while the  $C_6H_4$  and  $C_{2n}H_6$  ( $n=4, 5, 6$ ) fluxes are less dependent on the  $C_2H_2$  gas fraction. Indeed, the  $C_{2n}H_2$  are mainly formed by  $C_2H$  insertion into  $C_{2n-2}H_2$ , which results in similar trends of the  $C_{2n}H_2$  fluxes, whereas the

$C_6H_4$  and  $C_{2n}H_6$  species are formed by neutralization of the corresponding ions on the wall. The H atom flux drops significantly with rising  $C_2H_2$  fraction (and hence decreasing  $H_2$  fraction), whereas the  $C_{2n}H_3$  fluxes reach a maximum at about 40%  $C_2H_2$ . Indeed, these radicals are mainly produced by H insertion into  $C_{2n}H_2$ , and the decreasing trend of the H flux upon increasing  $C_2H_2$  fraction, in combination with the increasing trend for the  $C_{2n}H_2$  flux, results in a maximum at an intermediate  $C_2H_2$  fraction of 40%.

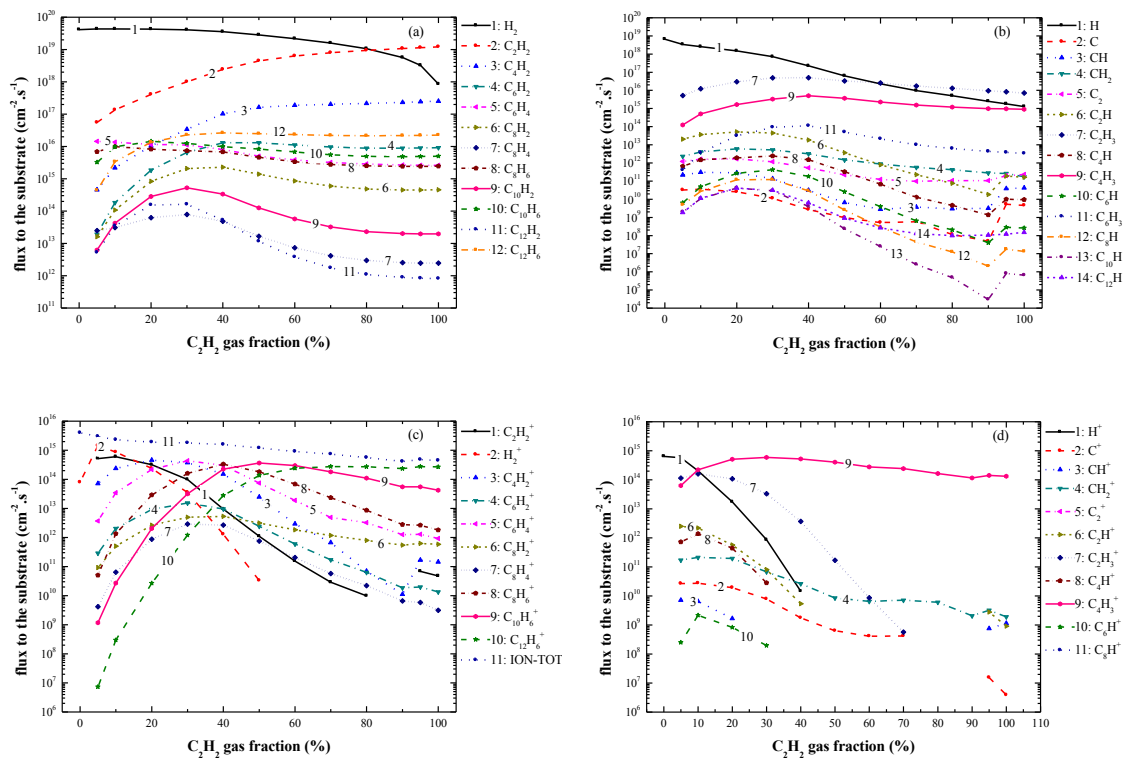


Figure 2: Calculated radially-averaged fluxes of the various molecules (a), radicals (b) and ions (c,d) bombarding the substrate, as a function of the  $C_2H_2$  gas fraction, for the  $C_2H_2/H_2$  gas mixture. The other operating conditions are the same as in figure 1.

With respect to the ions, it is clear from figure 2(c,d) that the lighter ions, such as  $H^+$ ,  $H_2^+$ ,  $C_2H_2^+$  and  $C_2H_3^+$ , are predominant under  $H_2$ -rich conditions, whereas the heavier ions, such as  $C_{10}H_6^+$  and  $C_{12}H_6^+$ , turn to be important under  $C_2H_2$ -rich conditions.  $C_4H_3^+$  is characterized by a high flux for all gas fractions (see figure 2(d)), suggesting that this ion might be important in the CNT growth for the conditions under study. It is stated that hydrocarbon ions play a key role in the formation of amorphous carbon films [29]. Therefore, the fact that the larger hydrocarbon ions are predominant under  $C_2H_2$ -rich conditions might explain why these conditions are not so often used for CNT growth, and that most experiments are performed for a  $C_2H_2$  fraction below 20% (e.g., [8,9,20]).

Finally, it is worth to mention that atomic carbon is hardly formed in the plasma (see figure 2(b)). Therefore, we can conclude that the carbon sources for CNT growth arise mainly from the decomposition of hydrocarbon molecules and radicals on the catalyst surface, as is also stated in [30].

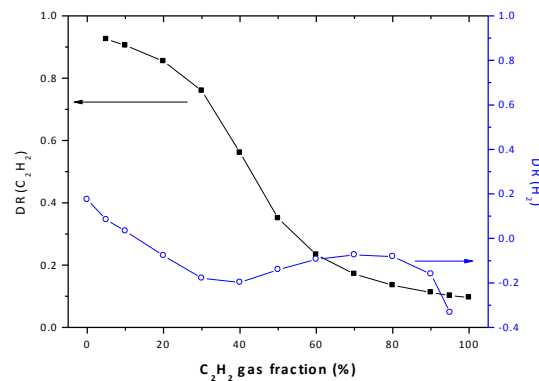


Figure 3: Calculated decomposition rates (DR) of the feedstock gas molecules ( $C_2H_2$  and  $H_2$ ), as a function of the  $C_2H_2$  gas fraction, for the  $C_2H_2/H_2$  gas mixture. The other operating conditions are the same as in figure 1.

Figure 3 illustrates the calculated decomposition rate (DR) of both background gases ( $C_2H_2$  and  $H_2$ ) in the plasma, as a function of  $C_2H_2$  fraction. The DR is defined as follows:

$$DR = 1 - \frac{\text{volume-averaged density of background gas}}{\text{density of background gas at inlet}}$$

Hence, a DR of 1 indicates 100% decomposition, or conversion into other species.  $C_2H_2$  has a high DR at low  $C_2H_2$  gas fraction (see left axis), and the DR drops significantly upon increasing  $C_2H_2$  fraction, especially in the range between 30 and 70%. The  $C_2H_2$  species are believed to be the main precursors for CNT growth in a PE-CVD system [10,12]. Hence, a high DR of  $C_2H_2$ , in combination with a low  $C_2H_2$  fraction in the gas mixture, gives rise to a low  $C_2H_2$  flux to the substrate, which might suggest a relatively low (and hence: controlled) growth rate for the CNTs. This is indeed observed experimentally [9,20]. The DR of  $H_2$  is found to be very low at low  $C_2H_2$  fraction, and it is even negative at  $C_2H_2$ -rich conditions, as is obvious from figure 3 (right axis). These negative values for the DR indicate that more  $H_2$  molecules are formed, e.g., out of  $C_2H_2$ , rather than decomposed.

### 3.3. Comparison of $H_2$ and $NH_3$ as dilution gases

When  $NH_3$  is used as the dilution gas instead of  $H_2$ , some new species appear in the plasma, as is clear from Table 2 above. Figure 4 illustrates the fluxes of these extra species towards the substrate, as a function of the  $C_2H_2$  gas fraction.  $N_2$ ,  $N_2H_2$  and  $NH_4^+$  appear to be important neutrals and ions, respectively, besides the background gases  $C_2H_2$  and  $NH_3$ . It was reported [25] that the presence of  $N_2$  can enhance carbon diffusion into the catalyst, promoting CNT growth. Hence, this might explain why in many papers (e.g., [8-10,12,24])  $NH_3$  is used as the dilution gas, rather than  $H_2$ .

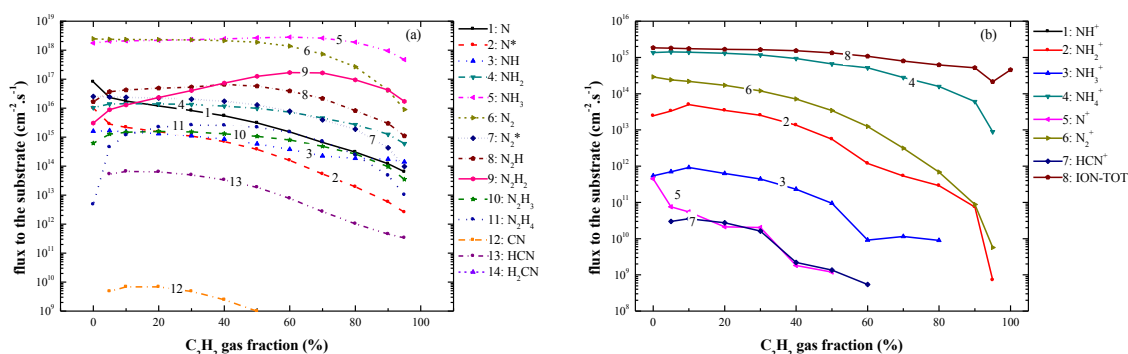


Figure 4: Calculated radially-averaged fluxes of the extra neutral species (a) and ions (b) bombarding the substrate, as a function of the  $C_2H_2$  gas fraction, for the  $C_2H_2/NH_3$  gas mixture. The other operating conditions are the same as in figure 1.

The DRs of  $C_2H_2$  and  $NH_3$  are plotted against  $C_2H_2$  fraction in figure 5. The DR of  $C_2H_2$  shows the same trend as in the  $C_2H_2/H_2$  gas mixture (cf. figure 3 above). Moreover, the DR of  $NH_3$  drops also from nearly 1 at low  $C_2H_2$  gas fraction to values around 0.4 at high  $C_2H_2$  fraction. This leads to a pronounced drop in the atomic H production. It is generally known that H can etch away amorphous carbon phases formed in the growing CNTs [20]. Therefore, the large flux of H atoms at low  $C_2H_2$  gas fraction, in combination with the low fluxes of hydrocarbon ions towards the substrate, suggests that “clean” CNT growth conditions can be achieved at a low  $C_2H_2$  gas fraction. This is also reported in literature. Indeed, Chowalla et al. [8] found that CNTs could be grown at a  $C_2H_2$  fraction between 5 and 30%. Also in [24] the longest CNTs with the highest density were obtained for the smallest  $C_2H_2/NH_3$  gas ratio (15/150), corresponding to around 10% of  $C_2H_2$ .

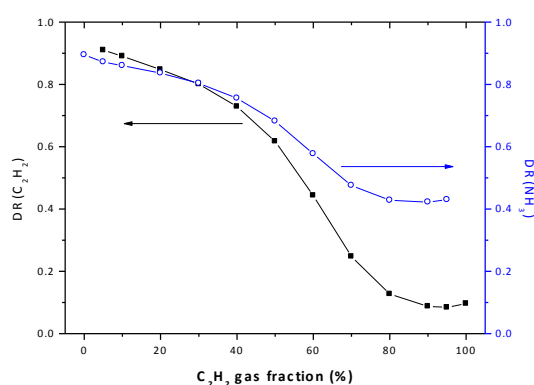


Figure 5: Calculated decomposition rates (DR) of the feedstock gas molecules ( $C_2H_2$  and  $NH_3$ ), as a function of the  $C_2H_2$  gas fraction, for the  $C_2H_2/NH_3$  gas mixture. The other operating conditions are the same as in figure 1.

## 5. Conclusions

We have applied a hybrid model to investigate the plasma chemistry in an ICP reactor in  $C_2H_2/H_2$  and  $C_2H_2/NH_3$  gas mixtures. First, some general calculation results were illustrated, such as the power density, electron and gas temperature, electron density



and densities of some other plasma species. Subsequently, the fluxes of the various plasma species bombarding the substrate, as well as the decomposition rates (DRs) of the feedstock gases were analyzed for different  $C_2H_2/H_2$  and  $C_2H_2/NH_3$  gas ratios.

It is found that both gas mixtures give rise to a very rich plasma chemistry, with several large hydrocarbon molecules, radicals and ions, especially at a high  $C_2H_2$  gas fraction. When  $NH_3$  is applied as the dilution gas,  $N_2$ ,  $N_2H$  and  $N_2H_2$ , as well as  $NH_4^+$ , are also important plasma species. The C flux, on the other hand, was found to be the lowest of all radicals, which confirms that the carbon source for CNT growth mainly arises from the decomposition of hydrocarbon molecules on the catalyst surface [30].

The calculated DRs of the feedstock gas molecules illustrate that  $C_2H_2$  is almost fully decomposed at low  $C_2H_2$  fraction in both gas mixtures, but the DR drops significantly upon higher  $C_2H_2$  gas fraction. The DR of  $H_2$  was found to be very low, or even negative at a  $C_2H_2$  fraction above 10%, indicating that more  $H_2$  molecules are formed (out of e.g.,  $C_2H_2$ ), rather than decomposed. The DR of  $NH_3$  follows a similar trend as the  $C_2H_2$  DR, being high at low  $C_2H_2$  fraction, and decreasing for higher  $C_2H_2$  fractions. This results in a drop of the atomic H flux towards the substrate (or the growing CNT) at high  $C_2H_2$  fraction. Moreover, the higher hydrocarbon fluxes also exhibit a maximum at these conditions. Therefore, we expect that an amorphous carbon film will be formed under these conditions, which cannot easily be etched away, because of the low amount of etching H atoms, and this will suppress the growth of CNTs. Hence, we expect that a low fraction of  $C_2H_2$  and hence a higher fraction of  $H_2$  or  $NH_3$  in the gas mixture will result in more “clean” conditions for CNT growth. Indeed, experiments reported in literature appear to be performed typically at a  $C_2H_2$  fraction below 20% (e.g., [8,9,20]).

### Acknowledgements

The Fund for Scientific Research (FWO Flanders) and the Prime Minister's Office through IAP-VI are acknowledged for financial support. The calculations were performed on the CalcUA computing facilities of the University of Antwerp. We are also very grateful to M. Kushner and group members from providing the HP-EM and useful advice.

### References

- [1] Tseng G Y and Ellenbogen J C 2001 *Science* **294** 1293-4.
- [2] Darkrim F L, Malbrunot P and Tartaglia G P 2002 *Int J Hydrogen Energ* **27** 193-202.
- [3] Guillorn M A, Melechko A V, Merkulov V I, Ellis E D, Simpson M L, Baylor L R and Bordonaro G J 2001 *J Vac Sci Technol B* **19** 2598-601.
- [4] Journet C, Maser W K, Bernier P, Loiseau A, delaChapelle M L, Lefrant S, Deniard P, Lee R and Fischer J E 1997 *Nature* **388** 756-8.
- [5] Yudasaka M, Komatsu T, Ichihashi T and Iijima S 1997 *Chemical Physics Letters* **278** 102-6.
- [6] Lee C J, Kim D W, Lee T J, Choi Y C, Park Y S, Lee Y H, Choi W B, Lee N S, Park G S and Kim J M 1999 *Chemical Physics Letters* **312** 461-8.
- [7] Cassell A M, Ye Q, Cruden B A, Li J, Sarrazin P C, Ng H T, Han J and Meyyappan M 2004 *Nanotechnology* **15** 9-15.

- [8] Chhowalla M, Teo K B K, Ducati C, Rupesinghe N L, Amaratunga G A J, Ferrari A C, Roy D, Robertson J and Milne W I 2001 *J Appl Phys* **90** 5308-17.
- [9] Bell M S, Lacerda R G, Teo K B K, Rupesinghe N L, Amaratunga G A J, Milne W I and Chhowalla M 2004 *Appl Phys Lett* **85** 1137-9.
- [10] Bell M S, Teo K B K and Milne W I 2007 *J Phys D Appl Phys* **40** 2285-92.
- [11] Hash D, Bose D, Govindan T R and Meyyappan M 2003 *J Appl Phys* **93** 6284-90.
- [12] Bell M S, Teo K B K, Lacerda R G, Milne W I, Hash D B and Meyyappan M 2006 *Pure Appl Chem* **78** 1117-25.
- [13] Okita A, Suda Y, Ozeki A, Sugawara H, Sakai Y, Oda A and Nakamura J 2006 *J Appl Phys* **99** 0143021-7.
- [14] Okita A, Suda Y, Oda A, Nakamura J, Ozeki A, Bhattacharyya K, Sugawara H and Sakai Y 2007 *Carbon* **45** 1518-26.
- [15] Oda A, Suda Y and Okita A 2008 *Thin Solid Films* **516** 6570-4.
- [16] Delzeit L, McAninch I, Cruden B A, Hash D, Chen B, Han J and Meyyappan M 2002 *J Appl Phys* **91** 6027-33.
- [17] Meyyappan M, Delzeit L, Cassell A and Hash D 2003 *Plasma Sources Sci T* **12** 205-16.
- [18] Cruden B A and Meyyappan M 2005 *J Appl Phys* **97**-84311-15.
- [19] Wei H W 2008 Study of Growth of Vertically-Aligned Carbon Nanofibers by Plasma Enhanced Chemical Vapor Deposition-Growth Mechanism and Field Emission. In: *Department of Engineering and System Science*, (Hsinchu, Taiwan: National Tsing Hua University) p 175.
- [20] Lin Y Y, Wei H W, Leou K C, Lin H, Tung C H, Wei M T, Lin C and Tsai C H 2006 *J Vac Sci Technol B* **24** 97-103.
- [21] Wei H W, Leou K C, Wei M T, Lin Y Y and Tsai C H 2005 *J Appl Phys* **98** 044313.
- [22] Yang C S 2005 Low temperature growth of single-walled carbon nanotubes by PECVD. In: *Department of Engineering and System Science*, (Hsinchu, Taiwan: National Tsing Hua University) p 88.
- [23] Maschmann M R, Amama P B, Goyal A, Iqbal Z, Gat R, Fisher T S, 2006 *Carbon* **44** 10-18.
- [24] Wang P, Lu J and Zhou O 2008 *Nanotechnology* **19** 185605-1-7.
- [25] Lin C H, Chang H L, Hsu C M, Lo A Y and Kuo C T 2003 *Diam Relat Mater* **12** 1851-7.
- [26] Ventzek P L G, Sommerer T J, Hoekstra R J and Kushner M J 1993 *Appl Phys Lett* **63** 605-7.
- [27] Mao M and Bogaerts A 2010 *J Phys D Appl Phys* **43** 205201-1-20.
- [28] Mao M and Bogaerts A *J Phys D Appl Phys* (submitted).
- [29] Grigonis A, Sablinskas V, Silinskas M and Tribandis D 2004 *Vacuum* **75** 261-7.
- [30] Hofmann S, Sharma R, Ducati C, Du G, Mattevi C, Cepek C, Cantoro M, Pisana S, Parvez A, Cervantes-Sodi F, Ferrari A C, Dunin-Borkowski R, Lizzit S, Petaccia L, Goldoni A and Robertson J 2007 *Nano Lett* **7** 602-8.